

Optimization on Operating Parameters of a Small-Scale CCHP System Based on Economic- Energy Efficiency

Yuchen Dai ^{a,b}, Handong Wang ^{a,*}

^a*School of M & E, Shenzhen Polytechnic, Shenzhen 518000, China*

^b*School of Science, Wuhan Institute of Technology, Wuhan 430205, China*

Corresponding author. Tel./fax: 0755-26731327 E-mail address: zlwhtd@szpt.edu.cn (Wang HD)

Abstract — A small-scale combined cooling, heating and power (CCHP) system with a novel NH₃/LiNO₃/He diffusion absorption refrigeration (DAR) is proposed and the performance of the CCHP system is simulated and analyzed. The results based on using economic-exergy efficiency (η_{ecex}) as the evaluation criterion show that the economic-exergy performance of the CCHP system is mainly affected by the inlet temperature ($T_{expa,inlet}$) and inlet pressure ($P_{expa,inlet}$) of screw expander, the temperature difference of the generator of DAR (ΔT_{gene}) and the solution recirculation ratio (rr) of DAR system. However, in those mentioned parameters, the influence characteristics on economic-exergy performance are not exactly the same due to the different effects of the working conditions. Genetic algorithm (GA) is employed to achieve the highest economic-exergy efficiency in the optimization of the system operating in “following the electricity loads” mode. The optimization result indicates that, within the range of decision variables, the economic-exergy efficiency can achieve 23.08% when the four key parameters, namely screw expander inlet temperature, screw expander inlet pressure, temperature difference of the generator of DAR and solution recirculation ratio are 179.95oC, 693.68kPa, 5.03oC, 0.699, respectively.

Key words - CCHP; diffusion absorption refrigeration; economic-exergy; optimization

I. INTRODUCTION

The combined cooling, heating and power (CCHP) system, which is built on the basis of energy cascade utilization, can provide cooling, heating and power simultaneously. It can not only achieve the purpose of energy efficiency, but reduce the dependence on the power grid to secure the safety of power operation. Thus, it gains many more attentions by researchers all over the world. Numerous studies on CCHP have been involved in many aspects of system performance. To design the system structure and obtain the optimal operating parameters, many researchers have worked on the CCHP system optimization studies from the aspects of thermodynamic, economy and environment etc. Wang et al. [1] proposed a novel CCHP system driven by solar energy and used GA method to optimize the system using the exergy efficiency as the objective function. Wang et al. [2,3] combined a Brayton cycle and transcritical CO₂ refrigeration cycle to perform a CCHP driven by solar energy. Genetic algorithm was also employed to carry out the system optimization with modified system efficiency or exergy efficiency as the objective function.

Parametric analysis was conducted to track the operation performance and to analyze the influence of several key thermodynamic parameters namely turbine inlet

temperature, turbine inlet pressure, turbine back pressure,

Nomenclature			
COP	coefficient of performance	cool	cooling
f	solution circulation ratio	ecex	economic-exergy
h	enthalpy, kJ/kg	evap	evaporator in DAR system
m	mass flow rate, kg/s	expa	screw expander
P	pressure, kPa	gene	the generator of DAR
Q	heat rate, kW	heat	heating
rr	solution recirculation ratio	in	inlet CCHP system
T	temperature, °C	inlet	inlet expander
X	vapor dryness	l	liquid
x	mass concentration of ammonia in lithium nitrate ammonia solution	PHE	plate heat exchanger
		power	power
		pump	cycle pumps in CCHP system
	<i>Greek letters</i>	ratio	the proportion of using vapor dryness
β	the ratio of the price	s	isentropic point
η	efficiency, %	sc	solution cooler
ΔT	temperature difference, °C	shx	solution heat exchanger
		strong	strong ammonia solution
	<i>subscripts</i>	sv	superheated vapor
CCHP	CCHP system	s2	the saturation point of ammonia under a pressure
P		v	vapor
cc	condenser in DAR system	weak	weak ammonia solution
cond	condenser in CCHP system		

ejector inlet temperature, ejector back pressure and

respective temperature. 7) The energy consumption of each pump in DAR system is negligible. 8) The DAR system pressure is the saturated ammonia pressure under condenser temperature. 9) The temperature difference at low temperature side of solution heat exchanger is 3°C. 10) The temperature difference between inlet and outlet of cooling heat exchanger is 5°C.

B. The Equations Of Physical Properties

The thermodynamic properties of water are calculated by

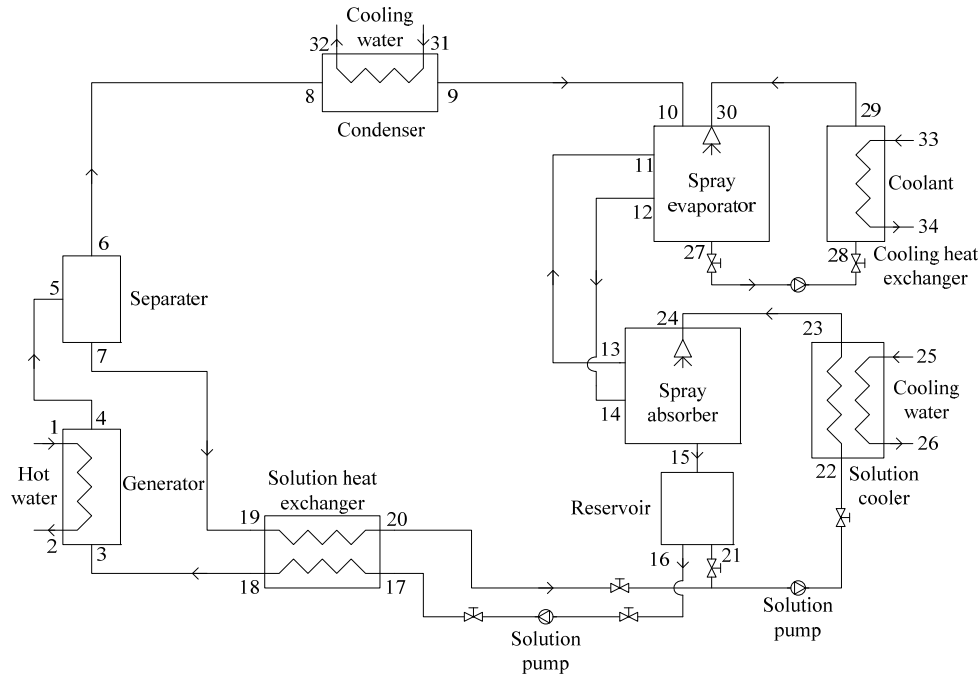


Fig.2 Diagram of flow chart of the diffusion absorption refrigeration system

The pressure-temperature equation of pure ammonia under vapor-liquid equilibrium, enthalpy equation of liquid ammonia and saturated ammonia vapor can be given by Ref. [13]:

$$P(T) = 10^3 \sum_{i=0}^6 a_i T^i \quad (1)$$

$$h_l(T) = \sum_{i=0}^6 b_i T^i \quad (2)$$

$$h_v(T) = \sum_{i=0}^6 c_i T^i \quad (3)$$

The P - T - x balance equation of NH_3 - LiNO_3 solution:

$$\ln P = A + \frac{B}{T} \quad (4)$$

REFPROP 9.01 [12] developed by the National Institute of Standards and Technology of the United States. As for the ternary working fluids in the DAR system, the thermodynamic properties are all provided by references. Helium is only the diffusion gas to balance the pressure in the DAR system.

Where $A = 16.29 + 3.859(1-x)^3$;

$$B = -2802 - 4192(1-x)^3 .$$

The h - T - x balance equation of NH_3 - LiNO_3 solution [14]

;

$$h(T, x) = A + BT + CT^2 + DT^3 \quad (5)$$

Where

$$A = \begin{cases} -215 + 1570(0.54 - x)^2 & x < 0.54 \\ -215 + 689(x - 0.54)^2 & x > 0.54 \end{cases} ;$$

$$B = 1.15125 + 3.382678x ;$$

$$C = (1.099 + 2.3965x) \cdot 10^{-3} ; D = 3.93333 \cdot 10^{-5} x .$$

The enthalpy equation of superheated ammonia vapor [15]:

$$h_{sv} = 2.68T - 1.64T_{s2} + 1440 \quad (6)$$

C. Calculation Models

According to the quality and energy conservation of each component, the calculation models can be obtained as follows:

1) CCHP system

The subscripts 1, 2, 3...12 are state points in Fig.1.

Vapor generator

$$Q_{in} = m_{CCHP}(h_2 - h_1) \quad (7)$$

Screw expander

$$Q_{power} = m_{CCHP}\eta_{expa,s}(h_3 - h_{4s}) \quad (8)$$

Heater

$$Q_{heat} = m_{CCHP}\eta_{PHE}(h_7 - h_8) \quad (9)$$

Condenser

$$Q_{cond} = m_{CCHP}\eta_{PHE}(h_9 - h_{10}) \quad (10)$$

Cycle pump

$$Q_{pump} = m_{CCHP}(h_{12s} - h_{11}) / \eta_{pump,s} \quad (11)$$

2) DAR system

The subscripts 1, 2, 3...12 are state points in Fig.(2).

Generator of DAR

$$Q_{gene} = m_4h_4 - m_3h_3 \quad (12)$$

Separator

$$m_3h_5 = m_6h_6 + m_7h_7 \quad (13)$$

$$m_5x_{strong} - m_6 - m_7x_{weak} = 0 \quad (14)$$

Condenser

$$Q_{cc} = m_8(h_9 - h_8) \quad (15)$$

$$m_{10} + m_{11} = m_{12} \quad (16)$$

$$m_{10} + m_{11}x_{11} = m_{12}x_{12} \quad (17)$$

$$m_{10}h_{10} + m_{11}h_{11} + m_{30}h_{30} = m_{12}h_{12} + m_{27}h_{27} \quad (18)$$

$$Q_{evap} = m_{27}(h_{30} - h_{27}) \quad (19)$$

Adiabatic spray absorber

$$m_{14} + m_{24} = m_{13} + m_{15} \quad (20)$$

$$m_{14}x_{14} + m_{24}x_{24} = m_{13}x_{13} + m_{15}x_{15} \quad (21)$$

$$m_{14}h_{14} + m_{24}h_{24} = m_{13}h_{13} + m_{15}h_{15} \quad (22)$$

Reservoir

$$m_{15} = m_{16} + m_{21} \quad (23)$$

$$m_{15}h_{15} = m_{16}h_{16} + m_{21}h_{21} \quad (24)$$

Solution cooler and Solution heat exchanger

$$m_{20}(h_{19} - h_{20}) = \eta_{shx}m_{18}(h_{18} - h_{17}) \quad (25)$$

$$m_{22}\eta_{sc}(h_{23} - h_{22}) = m_{26}(h_{25} - h_{26}) \quad (26)$$

Coefficient of performance, solution circulation ratio and solution recirculation ratio

$$COP = \frac{Q_{evap}}{Q_{gene}} \quad (27)$$

$$f = \frac{1 - x_{weak}}{x_{strong} - x_{weak}} \quad (28)$$

$$rr = \frac{m_{21}}{m_{20}} \quad (29)$$

3) Economic-exergy efficiency

$$\eta_{ecex} = \frac{Q_{power} + \beta_{cool}Q_{cool} + \beta_{heat}Q_{heat}}{Q_{in}} \quad (30)$$

The average price of commercial power supply, cooling supply and heating supply is 0.623 yuan/kWh, 0.218 yuan/kWh and 0.191 yuan/kWh, respectively [16]. Thus, the price ratio factor can be drawn as: $\beta_{cool}=0.35$; $\beta_{heat}=0.307$.

IV. SIMULATION RESULTS AND DISCUSSIONS

By applying the above physical equations and calculation models, the relationships among the ratio of vapor dryness used by DAR ($X_{cool, ratio}$), screw expander inlet temperature ($T_{expa, inlet}$), screw expander inlet pressure ($P_{expa, inlet}$), temperature difference of the generator of DAR (ΔT_{gene}), solution recirculation ratio of DAR system (rr) and economic-exergy efficiency (η_{ecex}) of the CCHP system have been simulated and calculated.

The CCHP system in this paper is a small-scale system which has a small system capacity. Thus, the power capacity is set to be the maximum load 10kW while simulating. The evaporator temperature of DAR system is set to be -15°C to reflect the characteristic of the DAR system that it can produce the low temperature. The hot water temperature of heater is set to be domestic water temperature 60°C. In the parameters sensitivity analysis, when a parameter value changes, other parameters value remains unchanged in Table I.

In order to utmostly utilize the waste heat of exhaust vapor from the screw expander under “following the electricity loads” mode, the vapor dryness is completely

used by DAR and heating. The temperature of working fluid water is also set to be 10°C of sub-cooling temperature to make sure the working fluid water is completely condensed after heater, which also can save off a condenser of the CCHP system.

TABLE I. SIMULATION PARAMETERS OF THE CCHP SYSTEM

Term	value
Ratio of vapor dryness used by DAR	0.5
Screw expander inlet temperature/°C	160
Screw expander inlet pressure/kPa	600
Temperature difference of the generator of DAR/°C	10
Solution recirculation ratio of DAR system	1

The relationships among $X_{cool,ratio}$, Q_{cool} , Q_{heat} and η_{ecex} are shown in Fig. (3). Obviously, Q_{cool} increases and Q_{heat} decreases as $X_{cool,ratio}$ increases. The η_{ecex} also decreases due to the low *COP* which is caused by the low evaporator temperature. The $X_{cool,ratio}$ can be commanded by adjusting the mass flow rate of cooling and heating when the CCHP system is running. However, it is worth mentioning that the $X_{cool,ratio}$ is commanded according to the cooling or heating demand of users. Thus, it is inappropriate to minimize the $X_{cool,ratio}$ to increase the η_{ecex} . Besides, it is not suitable to select the $X_{cool,ratio}$ as a decision variable.

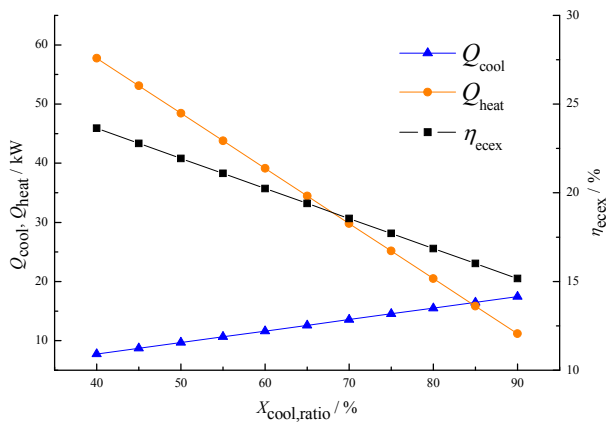


Fig.3 The relationships among the $X_{cool,ratio}$ and cooling capacity, heating capacity and economic-exergy efficiency

Fig. (4). shows the effects of $T_{expa,inlet}$ on Q_{cool} , Q_{heat} and η_{ecex} . It is not evident that the trends of Q_{cool} , Q_{heat} and η_{ecex} changes as $T_{expa,inlet}$ increases. This is because that the $T_{expa,inlet}$ should be higher than the saturation temperature under 600kPa of $P_{expa,inlet}$. And as a small-scale system, the heat source temperature is not high enough. Thus, the consideration range of $T_{expa,inlet}$ is not very large and the η_{ecex} changes not obviously among the range. Even so, it also can be found that the η_{ecex} increases slightly as $T_{expa,inlet}$ increases.

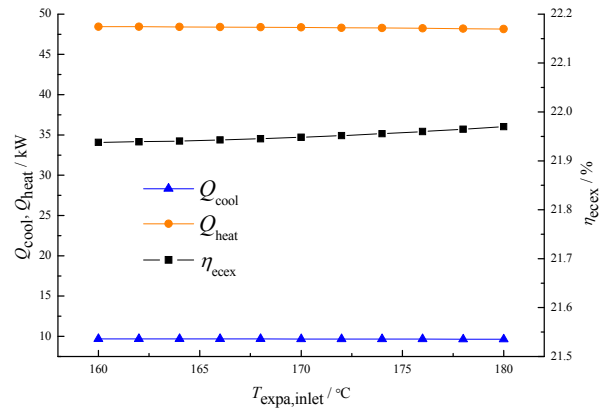


Fig.4 The relationships among the screw expander inlet temperature and cooling capacity, heating capacity and economic-exergy efficiency

Fig. (5) shows the effect of $P_{expa,inlet}$ on Q_{cool} , Q_{heat} , η_{ecex} and Q_{in} etc. It can be seen that there is a sudden jump section in the change process of the Q_{cool} , Q_{heat} , Q_{in} and m_{CCHP} as $P_{expa,inlet}$ increases. This is because that the saturation pressure of water is 618kPa when the screw expander inlet temperature is 160°C. And the water will be in two-phase region when the $P_{expa,inlet}$ exceeds the pressure point, which means the enthalpy of water drops significantly due to the latent heat of water vapor. And in order to achieve the set 10kW power generation under the situation, the mass flow rate load of the CCHP system will increase significantly, which leads to the significant increase of the Q_{cool} , Q_{heat} , Q_{in} . However, the degree of increase in Q_{cool} and Q_{heat} is less than the increase of Q_{in} . Thus, the η_{ecex} decreases significantly in that section. It also can be found in Fig.4 that the η_{ecex} increases obviously before that section as $P_{expa,inlet}$ increases. This is because that the water is approaching saturation point from superheated state as $P_{expa,inlet}$ increases before saturation point. And the Q_{cool} , Q_{heat} and Q_{in} decrease simultaneously in the process. But the degree of decrease in Q_{cool} and Q_{heat} is less than the decrease of Q_{in} , which comprehensively leads to the increasing of the η_{ecex} . Thus, the $P_{expa,inlet}$ should be approaching the saturation point instead of exceeding the saturation point.

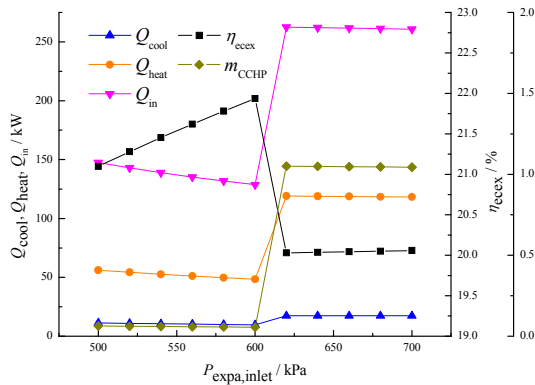


Fig.5 The relationships among the screw expander inlet pressure and cooling capacity, heating capacity and economic-exergy efficiency etc.

Fig. (6) shows the effect of ΔT_{gene} on Q_{cool} , m_{cool} and η_{ecex} . As the ΔT_{gene} increases, the m_{cool} increases while the Q_{cool} and η_{ecex} both decrease and the trends of Q_{cool} and η_{ecex} is almost the same. This is because that the generating temperature of the generator in DAR system decreases as ΔT_{gene} increases, resulting in a decrease in COP of DAR system. And the decrease of Q_{cool} is the major factor that leads to the decrease of η_{ecex} under the situation. Thus, it is advantageous to lower ΔT_{gene} while optimizing. But it is inappropriate to excessively lower ΔT_{gene} because the excessively lower ΔT_{gene} will increase the area of heat exchanger significantly which leads to increase the economic cost of system.

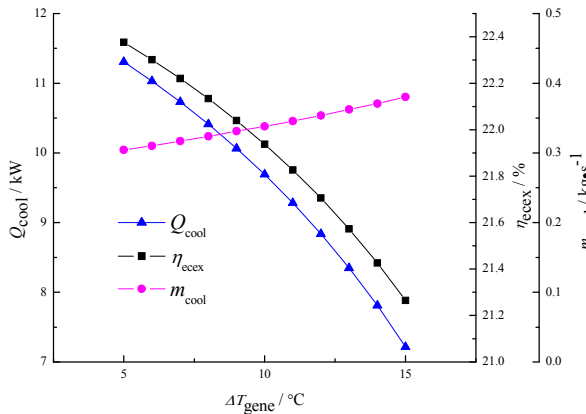


Fig.6 The relationships among temperature difference in generator of refrigeration system and cooling capacity, economic-exergy efficiency etc.

Fig. (7) shows the effect of rr on Q_{cool} , m_{cool} and η_{ecex} . The rr (recirculation ratio), defined as the ratio of the mass flow rate of the recirculated solution and the refrigerant mass flow rate (which is the ratio of m_{21} and m_{20} in Fig.2), will influence the concentration at the outlet of the absorber and some other parameters which leads to an effect on COP of

the DAR system to a certain extent. As shown in Fig. (7), with the increasing of rr , the m_{cool} increases while the Q_{cool} and η_{ecex} both appear decreasing trends after increasing. This is because that as the rr increases, the absorption temperature of the adiabatic absorber decreases while the spray concentration increases. And the COP of DAR system increases as the absorption temperature decreases and decreases as the spray concentration increases. A factor's increasing and the other factor's decreasing comprehensively leads to a decreasing trend after increasing of COP . And the trend of Q_{cool} is the major factor which leads to the trend of η_{ecex} under the situation. So the η_{ecex} shows a decreasing trend after increasing similarly. Though it can be found in Fig. (7) that there is an optimal value of rr on η_{ecex} , it is worth noting that this optimal value will change with the changing of the generating temperature of the generator in DAR system. And the generating temperature of the generator in DAR system is mainly effected by $T_{\text{expa,inlet}}$ and ΔT_{gene} . Thus, it is also necessary to select $T_{\text{expa,inlet}}$ and ΔT_{gene} as two factors of the decision variables after selecting rr as a decision variable.

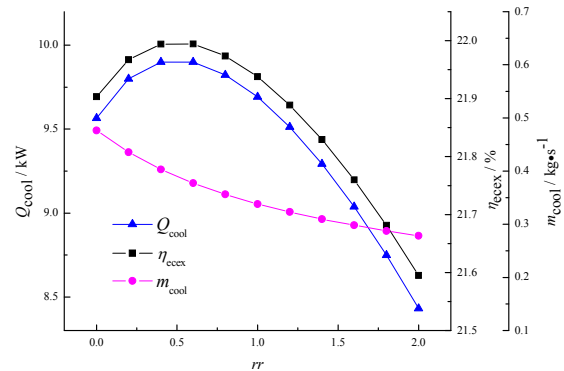


Fig.7 The relationships among recirculation ratio of the refrigeration system and cooling capacity, economic-exergy efficiency etc.

V. OPTIMIZATION RESULT

In order to obtain the values of several operating parameters under the optimal economic-exergy performance, the GA is employed to optimize the CCHP system. Four parameters namely $T_{\text{expa,inlet}}$, $P_{\text{expa,inlet}}$, ΔT_{gene} , rr are selected as decision variables under 50% $X_{\text{cool,ratio}}$ in “following the electricity loads” mode. Ranges for these decision variables as well as system constraints are summarized in Table II. The objective function is given by:

$$\max. \eta_{\text{ecex}} \left(T_{\text{expa,inlet}}, P_{\text{expa,inlet}}, \Delta T_{\text{gene}}, rr \right) \quad (31)$$

TABLE II. CONSTRAINTS AND RANGE OF DESIGN PARAMETERS FOR SYSTEM OPTIMIZATION

Constraint and design parameter range	Reason
$160^{\circ}\text{C} < T_{\text{expa,inlet}} < 180^{\circ}\text{C}$	Lowest and highest values of the screw expander inlet temperature
$500\text{kPa} < P_{\text{expa,inlet}} < 700\text{kPa}$	Lowest and highest values of the screw expander inlet pressure
$5^{\circ}\text{C} < \Delta T_{\text{gene}} < 15^{\circ}\text{C}$	Range of the temperature difference of the generator of DAR
$0 < rr < 2$	Range of the solution recirculation ratio
$Q_{\text{power}} = 10\text{kW}$	Power capacity limitation
$T_{\text{evap}} = -15^{\circ}\text{C}$	Evaporator temperature limitation of DAR system
$T_{\text{heat}} = 60^{\circ}\text{C}$	Heating temperature setting
$T_{\text{cc}} = 30^{\circ}\text{C}$	Condensing temperature setting of DAR system
$T_{\text{spray}} = 30^{\circ}\text{C}$	Spray temperature setting of the adiabatic absorber

The numerical values of the optimum decision variables and the optimal objective function obtained by single-objective are reported in TableIII.

TABLE III THE OPTIMIZATION RESULTS OF THE CCHP SYSTEM

Term	value
Screw expander inlet temperature/ $^{\circ}\text{C}$	179.95
Screw expander inlet pressure/kPa	693.68
Temperature difference of the generator of DAR/ $^{\circ}\text{C}$	5.03
Solution recirculation ratio of DAR system	0.699
Economic-exergy efficiency/%	23.08

It is obvious that the optimized $T_{\text{expa,inlet}}$ and ΔT_{gene} are almost endpoints of each range. This is because at the range of each decision variable, the η_{ecex} increases almost linearly as $T_{\text{expa,inlet}}$ increases or ΔT_{gene} decreases. It also can be seen that the optimized $P_{\text{expa,inlet}}$ is near value to its highest point. This is because that when the temperature of water is 179.95°C , its saturation pressure is 1001kPa which obviously exceeds the range of $P_{\text{expa,inlet}}$. As already mentioned above, the η_{ecex} increases as $P_{\text{expa,inlet}}$ increases before the saturation point. As for the rr , its optimized value is searched on the curve which appears a decreasing trend after increasing.

VI. CONCLUSIONS

In this paper, the simulation and optimization of a CCHP system with a novel DAR system are conducted. The main research (no.JCYJ20130331150226792).

conclusions drawn from present study are summarized as follows:

1) As the ratio of vapor dryness used by DAR increases, the cooling capacity increases while the heating capacity and the economic-exergy efficiency decreases. However, the ratio of vapor dryness used by DAR is commanded according to the cooling or heating demand of users when the CCHP system is running. Thus, it is inappropriate to select the ratio of vapor dryness used by DAR as a decision variable. As for the situation that the cooling or heating demand of users has been set, several key parameters namely screw expander inlet temperature, screw expander inlet pressure, temperature difference of the generator of DAR and solution recirculation ratio of DAR system are mainly factors to influence the economic-exergy efficiency of the CCHP system.

2) The economic-exergy efficiency of the CCHP system increases slightly as screw expander inlet temperature increases. The economic-exergy efficiency of the CCHP system increases significantly as screw expander inlet pressure increases before the saturation point. The economic-exergy efficiency of the CCHP system decreases linearly as the temperature difference of the generator of DAR increases. And the economic-exergy efficiency of the CCHP system appears a decreasing trend after increasing as the solution recirculation ratio of DAR system increases.

3) The system operates in “following the electricity loads” mode and the ratio of vapor dryness used by DAR is 50%. Screw expander inlet temperature, screw expander inlet pressure, temperature difference of the generator of DAR and solution recirculation ratio of DAR system are selected as the decision variables, while the economic-exergy efficiency is selected as the objective function for the optimization. GA is employed to achieve the optimum performance in the single-objective optimization. The optimization result shows that the economic-exergy efficiency can highest achieve 23.08% when the four key parameters namely screw expander inlet temperature, screw expander inlet pressure, temperature difference of the generator of DAR, solution recirculation ratio are 179.95°C , 693.68kPa , 5.03°C , 0.699 , respectively.

CONFLICT OF INTEREST

The authors confirm that this article content has no conflicts of interest.

ACKNOWLEDGMENT

The authors are grateful to Shenzhen Science and Technology Innovation Committee for supporting this

REFERENCES

- [1] Wang, J.J.; Jing, Y.Y.; Zhang, C.F. Optimization of capacity and operation for CCHP system by genetic algorithm .J. Applied Energy, 87,1325-1335, 2010.
- [2] Wang, J.F.; Dai, Y.P.; Gao, L.; Ma, S.L. A new combined cooling, heating and power system driven by solar energy .J. Renewable Energy, 34,2780-2788, 2009.
- [3] Wang, J.F.; Zhao, P.; Niu, X.Q.; Dai, Y.P. Parametric analysis of a new combined cooling, heating and power system with transcritical CO₂ driven by solar energy .J. Applied Energy, 94:58-64, 2012.
- [4] Wang, M.; Wang, J.F.; Zhao, P.; Dai, Y.P. Multi-objective optimization of a combined cooling, heating and power system driven by solar energy.J. Energy Conversion and Management, 89(2015):289-297.
- [5] Sepehr, S.; Ahmadreza, S. Optimization of combined cooling, heating and power generation by a solar system.J. Renewable Energy, 80(2015): 699-712.
- [6] Dominkovic', D.F.; C'osic', B.; Bac'elic' Medic', Z.; Duic', N. A hybrid optimization model of biomass trigeneration system combined with pit thermal energy storage.J. Energy Conversion and Management, 104(2015): 90-99.
- [7] Sadeghi, M.; Chitsaz, A.; Mahmoudi, S.M.S.; Rosen, M.A. Thermoeconomic optimization using an evolutionary algorithm of a trigeneration system driven by a solid oxide fuel cell.J. Energy, 89(2015): 191-204.
- [8] Feng, Z.B.; Jin, H.G. Performance assessment of combined cooling, heating and power.J. Journal of Engineering Thermophysics, 26(5): 725-728, 2005.
- [9] Wang, H.D; Hou, Z.J.; Zhan, X.L. Research on Integrated Fridge and Air-Conditioner System Driven by Solar Energy and Natural Gas: Selection of Working Fluids.J. Journal of Shenzhen Polytechnic, 8(1): 3-7, 2009.
- [10] Wang, H.D; Hou, Z.J.; Zhan, X.L. Integrated Multi-Functional Refrigeration System Driven by Solar Energy and Natural Gas: Performance Simulation.J. Journal of Shenzhen Polytechnic, 8(3): 3-7, 2009.
- [11] Wang, H.D. Performance Evaluation of a Small Scale Modular Solar Trigenration System.J. International Journal of Photoenergy:1-9, 2014.
- [12] NIST Standard Reference Database 23 [DB]. NIST thermodynamic and transport properties of refrigerants and refrigerant mixtures REFPROP, Version 9.01, 2013.
- [13] Sun, D.W. Comparison of the performances of NH₃-H₂O, NH₃-LiNO₃ and NH₃-NaSCN absorption refrigeration systems .J. Energy Conversion and Management, 39(5/6): 357-368, 1998.
- [14] Infante Ferrira, C.A. Thermodynamic and physical property date equations for ammonia-lithium nitrate and ammonia-sodium thiocyanate solutions.J. Solar Energy. 32(2): 231-236,1984.
- [15] KAUSHIK, S.C; KUMAR, R. Thermodynamic study of a two-stage vapour absorption refrigeration system using NH₃ refrigerant with liquid/solid absorbents.J. Energy Conversion and Management, 25(4): 427-431, 1985.
- [16] Li, B.K.; Zhang, W.Z.; Zheng, W.G. Research on CCHP system based on natural gas engine.J. Intelligent Measure, 4(2):64-67, 2015.